

# Izbira gladilne spremenljivke z optičnimi napetostnimi nanosi

## Choice of Smoothing Parameter Using Photo-Elastic Coatings

Violeta Kravčenkienė<sup>1</sup> - Algimantas Aleksa<sup>1</sup> - Minvydas Ragulskis<sup>1</sup> - Rimas Maskeliūnas<sup>2</sup>  
(<sup>1</sup> Kaunas University of Technology, Kaunas; <sup>2</sup> Vilnius Gediminas Technical University, Vilnius)

*V prispevku je opisana metoda izbire gladilne spremenljivke. Prikazana je na problemu fotoelastične analize upogibnih nihanj plošče. Model končnih elementov sistema temelji na aproksimaciji pomikov vozlišč, medtem ko na postavitev zunanjih robov vpliva polje napetosti v fotoelastičnem nanosu. Vzorci zunanjih robov, ki smo jih ustvarili brez glajenja, se na mejah med elementi vedejo nenaravno. V primeru, da je gladilna spremenljivka prevelika, dobimo preveč zglajeno sliko, ki sicer lahko izgleda sprejemljivo, vendar je daleč od resnične fotoelastične slike. Predstavljen način izbire optimalne gladilne spremenljivke je posplošen za dvorazsežne Lagrangeve končne elemente.*

© 2006 Strojniški vestnik. Vse pravice pridržane.

**(Ključne besede: spremenljivke zglajene, izbor spremenljivk, plošče, nihanja upogibna, analize fotoelastične)**

*A method of choosing a smoothing parameter is described and illustrated for the problem of a photo-elastic analysis of the bending vibrations of a plate. The finite-element model of the system is based on an approximation of the nodal displacements, while the formation of fringes is governed by the stress field in the photo-elastic coating. Without smoothing the reconstructed patterns of the fringes exhibit a non-physical behaviour at inter-element boundaries. When the smoothing parameter is too big, an over-smoothed image is obtained, which may look acceptable but be far from the realistic photo-elastic image. The presented strategy for the selection of the optimum smoothing parameter is generalised for two-dimensional Lagrange finite elements.*

© 2006 Journal of Mechanical Engineering. All rights reserved.

**(Keywords: smoothing parameters, parameter choice, plates, bending vibrations, photo-elastic coatings)**

### 0 INTRODUCTION

The problem of the bending vibrations of a plate is a common one in different engineering applications. This problem was analysed by using photo-elastic coatings in [1]. Photo-elastic coating [2] is a classical technique for stress analysis.

The coating has a negligible effect on the vibrations of the plate. First, the eigenmodes are calculated using the usual plate-bending element. The coating is thin and the plane displacements in the coating coincide with the displacements on the surface of the plate, and are the same through the thickness of the coating. The stresses in the coating are calculated assuming conditions of plane stress. The directions of the incident and the reflected light are almost perpendicular to the coating.

The conventional FEM would require unacceptably dense meshing to produce sufficiently

smooth photo-elastic patterns. Therefore, there is a need to smooth the generated photo-elastic fringe patterns representing the stress distribution, and which are calculated from the displacement distribution. The choice of the optimum value of the smoothing parameter is an important problem that is addressed in this paper.

### 1 CHOICE OF THE SMOOTHING PARAMETER

First, the eigenmodes of the plate are calculated by using a displacement formulation common in finite element analysis. Further,  $x$ ,  $y$  and  $z$  are used to denote the axes of the orthogonal Cartesian system of coordinates. The plate-bending element with the independent interpolation of the displacement  $w$  and the rotations about the appropriate axes  $\theta_x$  and  $\theta_y$  is used [3]. It is assumed that the plate performs vibrations according to the

eigenmode (the frequency of the excitation is about equal to the eigenfrequency of the corresponding eigenmode). The vibrations of the plate are registered stroboscopically when the structure is in the state of extreme deflections according to the eigenmode.

The nodal variables of the plate-bending element are the deflection of the plate  $w$ , the rotation of the plate about the  $x$  axis  $\theta_x$  and the rotation of the plate about the  $y$  axis  $\theta_y$ . It is assumed that in the plate  $v = -z\theta_x$  and  $u = z\theta_y$ , where  $u$  and  $v$  are the displacements of the plate in the  $x$  and  $y$  directions, respectively. Thus  $u = (h/2)\theta_y$  and  $v = -(h/2)\theta_x$  are the displacements on the surface of the plate, and  $h$  is the thickness of the plate.

The eigenmodes of the plate are obtained in the usual way, assuming that the coating has no effect on the motion of the plate.

The stresses in the coating are calculated as:

$$\{\sigma\} = [D_c][B]\{\delta\} \quad (1),$$

where:

$$[B] = \begin{bmatrix} 0 & 0 & \frac{\partial N_1}{\partial x} & \dots \\ 0 & -\frac{\partial N_1}{\partial y} & 0 & \dots \\ 0 & -\frac{\partial N_1}{\partial x} & \frac{\partial N_1}{\partial y} & \dots \end{bmatrix} \quad (2)$$

$$[D_c] = \frac{h}{2} \begin{bmatrix} \frac{E_c}{1-\nu_c^2} & \frac{E_c\nu_c}{1-\nu_c^2} & 0 \\ \frac{E_c\nu_c}{1-\nu_c^2} & \frac{E_c}{1-\nu_c^2} & 0 \\ 0 & 0 & \frac{E_c}{2(1+\nu_c)} \end{bmatrix} \quad (3)$$

and  $\{\sigma\}$  is the vector of the components of stresses  $\sigma_x$ ,  $\sigma_y$  and  $\tau_{xy}$ , assuming that the coating is in the state of plain stress;  $N_i$  is the  $i$ -th shape function of the finite element;  $E_c$  is the modulus of elasticity of the coating;  $\nu_c$  is the Poisson's ratio of the coating; and  $\{\delta\}$  is the vector of generalised displacements of the eigenmode.

The field of the components of stresses incorporating its smoothing is determined as described in detail in [4]. Furthermore,  $\{\delta_x\}$  denotes the vector of the nodal values of  $\sigma_x$ ;  $\{\delta_y\}$  denotes the vector of nodal values of  $\sigma_y$ ;  $\{\delta_{xy}\}$  denotes the vector of nodal values of  $\tau_{xy}$ . The nodal values  $\{\delta_x\}$ ,  $\{\delta_y\}$

and  $\{\delta_{xy}\}$  are obtained from the following systems of linear algebraic equations:

$$\begin{aligned} & \left( \sum_i \iint_{e_i} ([N]^T [N] + [B^*]^T \lambda [B^*]) dx dy \right) \cdot \{\delta_x\} = \\ & = \sum_i \iint_{e_i} [N]^T \sigma_x dx dy, \\ & \left( \sum_i \iint_{e_i} ([N]^T [N] + [B^*]^T \lambda [B^*]) dx dy \right) \cdot \{\delta_y\} = \quad (4) \\ & = \sum_i \iint_{e_i} [N]^T \sigma_y dx dy, \\ & \left( \sum_i \iint_{e_i} ([N]^T [N] + [B^*]^T \lambda [B^*]) dx dy \right) \cdot \{\delta_{xy}\} = \\ & = \sum_i \iint_{e_i} [N]^T \tau_{xy} dx dy, \end{aligned}$$

where  $[N]$  is the row of the shape functions of the finite element;  $[B^*]$  is the matrix of the derivatives of the shape functions (the first row with respect to  $x$ ; the second row with respect to  $y$ );  $\lambda$  is the smoothing parameter;  $e_i$  stands for the domain of the  $i$ -th finite element; summation denotes the direct stiffness procedure.

When the smoothing parameter is too small the reconstructed images are of unacceptable quality because of the non-physical behaviour of the stress field as a result of its calculation from the displacement formulation. When the parameter is too big an over-smoothed image is obtained, which may look acceptable but be far from the real photo-elastic image.

The problem is to determine the optimum value of the smoothing parameter  $\lambda$ . This can be solved for a one-dimensional problem with linear elements ([5] and [6]). In our problem  $\lambda$  corresponds to  $Ak$  in [6] and 1 corresponds to  $hp$  in [6]. Thus the condition derived in [6] in our notation takes the form:

$$\frac{\lambda}{l} > \frac{l}{6} \quad (5),$$

where  $l$  is the length of the one-dimensional element.

This gives the optimum value of the smoothing parameter:

$$\lambda \approx \frac{l^2}{6} \quad (6),$$

or the optimum element size:

$$l \approx \sqrt{6\lambda} \quad (7).$$

So in order to obtain results which appear acceptable it is necessary to increase the smoothing parameter or to apply a finer finite-element mesh, or both.

For one-dimensional Lagrange elements instead of  $l$  the maximum distance between the consecutive nodes is to be used and the optimum value of the smoothing parameter is determined from:

$$\lambda \approx \frac{l^2}{R} \quad (8),$$

or the optimum element size is determined from:

$$l \approx \sqrt{R\lambda} \quad (9),$$

where the value of the coefficient  $R$  is determined on the basis of numerical experiments for a given element order.

For two-dimensional Lagrange elements instead of  $l$  the following value in the equations (8) and (9) is to be used:

$$l = \max(l_\xi, l_\eta) \quad (10),$$

where  $l_\xi$  is the maximum distance between the consecutive nodes in the direction of the local  $\xi$  coordinate and  $l_\eta$  is the maximum distance between the consecutive nodes in the direction of the local  $\eta$  coordinate.

The vector of polarisation is assumed to be given as:

$$\{P\} = \begin{Bmatrix} \cos \alpha \\ \sin \alpha \end{Bmatrix} \quad (11),$$

where  $\alpha$  is the angle of the vector of polarisation with the  $x$  axis.

Furthermore, the quadratic Lagrange element is used. In order to calculate the distance between the first pair of consecutive nodes the mapping between the variable  $\xi \in [-1, 0]$  and  $\tilde{\xi} \in [-1, 1]$  is introduced:

$$\xi = \frac{\tilde{\xi} - 1}{2} \quad (12).$$

Then:

$$\int ds = \int_{-1}^0 \frac{ds}{d\xi} d\xi = \int_{-1}^1 \frac{ds}{d\tilde{\xi}} \frac{1}{2} d\tilde{\xi} \quad (13),$$

where:

$$\frac{ds}{d\tilde{\xi}} = \sqrt{\left(\frac{dx}{d\tilde{\xi}}\right)^2 + \left(\frac{dy}{d\tilde{\xi}}\right)^2} \quad (14),$$

and  $s$  denotes the length of the curve.

In order to calculate the distance between the next pair of consecutive nodes the mapping between the variable  $\xi \in [0, 1]$  and  $\tilde{\xi}$  is introduced:

$$\xi = \frac{\tilde{\xi} + 1}{2} \quad (15).$$

Then:

$$\int ds = \int_0^1 \frac{ds}{d\xi} d\xi = \int_{-1}^1 \frac{ds}{d\tilde{\xi}} \frac{1}{2} d\tilde{\xi} \quad (16),$$

where  $ds/d\tilde{\xi}$  is given by Equation (14).

The two-dimensional Lagrange element is shown in Fig. 1. Thus, the curve lengths between the consecutive nodes for the one-dimensional quadratic Lagrange element with the nodes 1, 2 and 3: 1 and 2, 2 and 3 are calculated. Then the curve lengths between the consecutive nodes for the one-dimensional quadratic Lagrange element with the nodes 4, 5 and 6: 4 and 5, 5 and 6 are calculated. Then the curve lengths between the consecutive nodes for the one-dimensional quadratic Lagrange element with the nodes 7, 8 and 9: 7 and 8, 8 and 9 are calculated. Then the curve lengths between the consecutive nodes for the one-dimensional quadratic Lagrange element with the nodes 1, 4 and 7: 1 and 4, 4 and 7 are calculated. Then the curve lengths between the consecutive nodes for the one-dimensional quadratic Lagrange element with the nodes 2, 5 and 8: 2 and 5, 5 and 8 are calculated. Then the curve lengths between the consecutive nodes for the one-dimensional quadratic Lagrange element with the nodes 3, 6 and 9: 3 and 6, 6 and 9 are calculated. These calculations are performed as described previously. Then the maximum distance between the consecutive nodes is determined and the smoothing parameter for the element is obtained from Equation (8).

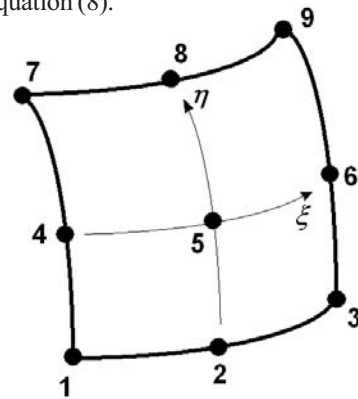


Fig. 1. Node numbering of the two-dimensional Lagrange quadratic finite element

## 2 RESULTS OF ANALYSIS

A circular plate with fixed internal radius performing harmonic vibrations according to the fourth eigenmode is analysed. It is considered that the plate is experiencing resonant vibrations on an eigenmode: the loading is assumed to be harmonic with the frequency of the eigenmode and not orthogonal to it.

The isolines of the absolute value of the difference of the principal stresses are presented in Fig. 2.

The lines of the principal directions of the stresses corresponding to the darkest parts from the images of the isoclinics (composite isoclinic pattern) are shown in Fig. 3. The composite isoclinic pattern is presented for the values of  $\alpha = (i-1)\pi/20$ , where  $i = 1, \dots, 10$ .

In order to investigate the effect of different values of the coefficient  $R$  the zoomed part of the

time averaged photo-elastic images for the plane polariscope with different values of  $R$  are presented in Fig. 4. It is evident that a smaller value of  $R$  gives bigger values of the smoothing parameter and thus a more realistic image.

## 3 CONCLUSIONS

The recommendations for the choice of the smoothing parameter in the smoothing procedure for the analysis of the bending vibrations of a plate by using photo-elastic coatings are presented.

As an illustration of the analysis the isolines of the absolute value of the difference of the principal stresses are obtained and the composite isoclinic pattern is produced. Those two drawings are the basis for the interpretation of the results of photo-elastic analysis.

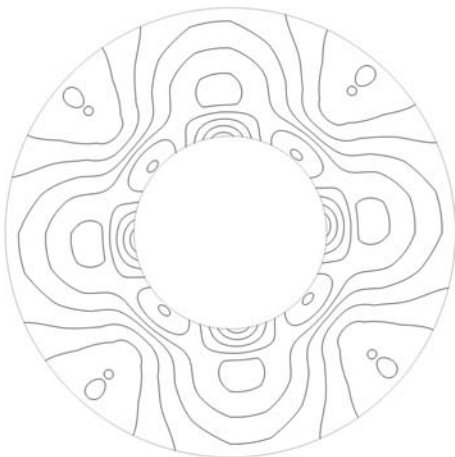
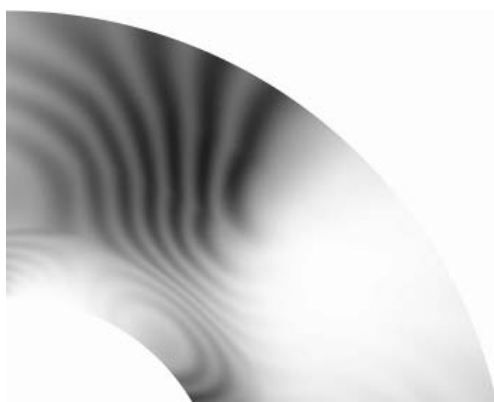


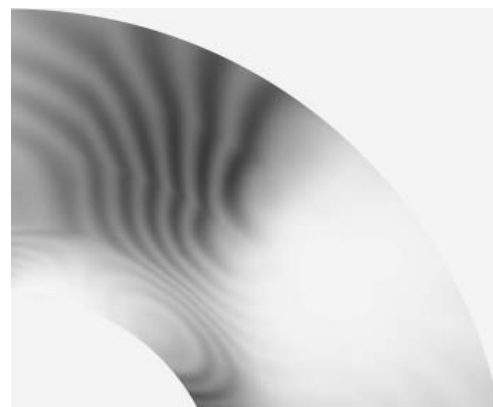
Fig. 2. Isolines of the absolute value of the difference of the principal stresses



Fig. 3. Composite isoclinic pattern for the values of  $\alpha = (i-1)\pi/20$ , where  $i = 1, \dots, 10$



a)



b)

Fig. 4. Zoomed time-averaged photo-elastic images for the plane polariscope with a)  $R=6$ , b)  $R=12$

4 REFERENCES

- [1] Saunoriene L., Ragulskis M., Maskeliunas R., Zubavičius L. (2005) Analysis of bending vibrations of a plate using photo-elastic coatings. *Journal of Vibroengineering*, 2005, Vol. 7(2), p. 1-6.
- [2] Kobayashi A. S. (1993) Handbook on experimental mechanics, Second Edition. *SEM*.
- [3] Bathe K. J. (1982) Finite element procedures in engineering analysis. P. 738. *Prentice-Hall*, New Jersey.
- [4] Ragulskis M., Ragulskis L. (2004) Plotting isoclinics for hybrid photoelasticity and FEM analysis. *Experimental Mechanics*. 2004. Vol. 44, No. 3. P. 235-240.
- [5] Ragulskis M., Kravčėnkiene V. (2005) Adaptive conjugate smoothing of discontinuous fields. Lecture Notes in Computer Science. 2005. Vol. 3401-0463. P. 463-470. *Springer Verlag*.
- [6] Barauskas R. (1998) Basis of the finite element method. P. 376. *Technologija*, Kaunas.

Authors' Addresses: Violeta Kravčėnkiene

Algiment Aleksa  
Prof.Dr. Minvydas Ragulskis  
Department of Mathematical Research in Systems  
Kaunas University of Technology  
Studentų str. 50, LT-51368  
Kaunas, Lithuania  
Minvydas.Ragulskis@ktu.lt

Dr. Rimas Maskeliunas  
Department of Printing Machines  
Vilnius Gediminas Technical University  
J. Basanaviciaus str. 28  
LT - 03224 Vilnius, Lithuania  
pgmas@me.vtu.lt

Prejeto:  
Received: 20.9.2005

Sprejeto:  
Accepted: 23.2.2006

Odrpto za diskusijo: 1 leto  
Open for discussion: 1 year